

# Polyisobutene/polystyrene interpenetrating polymer networks: Effects of network formation order and composition on the IPN architecture

Cédric Vancaeyzeele<sup>a</sup>, Odile Fichet<sup>a</sup>, Judith Laskar<sup>a</sup>,  
Sylvie Boileau<sup>b</sup>, Dominique Teyssié<sup>a,\*</sup>

<sup>a</sup> *Laboratoire de Physicochimie des Polymères et des Interfaces (LPPI), Université de Cergy-Pontoise-5, mail Gay-Lussac, Neuville-sur-Oise 95031 Cergy-Pontoise, Cedex, France*

<sup>b</sup> *Laboratoire de Recherche sur les Polymères, UMR 7581 CNRS, 2, rue H. Dunant, 94320 Thiais, France*

Received 10 November 2005; received in revised form 4 January 2006; accepted 11 January 2006

Available online 7 February 2006

## Abstract

In order to improve polyisobutene (PIB) mechanical properties, a PIB network is combined with a polystyrene (PS) one into an interpenetrating polymer network (IPN) architecture. PIB network is formed by alcohol addition between the hydroxyl end groups of a telechelic dihydroxy-polyisobutene and a pluri-isocyanate. PS network is synthesized by free-radical copolymerization of styrene with divinylbenzene. Thus, the optimal synthesis conditions are determined by FTIR spectroscopy and the kinetics of the alcohol–isocyanate addition is studied in detail. A short kinetic study of the PS network formation inside the PIB network is also carried out. The highest degree of interpenetration is obtained by forming the PIB network first. The corresponding transparent IPNs exhibit two mechanical relaxations corresponding to those of PS and PIB enriched phases. However, mechanical properties of PIB networks are tremendously improved by the presence of a PS network in such IPN architectures. © 2006 Elsevier Ltd. All rights reserved.

**Keywords:**  $\alpha,\omega$ -Dihydroxy polyisobutene; Polystyrene; Interpenetrating polymer network

## 1. Introduction

Combining elastomeric polymers with thermoplastic ones in a material is a real challenge. These combinations, which must be stable over time, can be obtained through the formation of blends or copolymers.

Block-type copolymers or thermoplastic elastomers (TPEs) display properties of conventional thermoset rubbers at room temperature and can be processed like conventional thermoplastics at high temperatures due to thermal reversible cross-links. TPEs are most often composed of microphases: hard phases determine the TPE mechanical strength, heat resistance, upper service temperature and strongly affect oil and solvent resistance. On the other hand, soft phases determine the elastomeric behavior and low temperature flexibility, thermal stability and aging resistance. The soft and hard phase weight ratio sets overall properties of those materials. However, the

physical cross-linking is easily deformed above the hard phase glass transition temperature and significant creep or even flow of the material can occur. Moreover, current TPEs do not show good resistance to common solvents.

Polyisobutene rubbers are well known to have special properties such as resistance to gas and moisture permeation, and high elasticity and flexibility at extreme temperatures particularly in the low range. Their glass transition temperatures can be as low as  $-76\text{ }^{\circ}\text{C}$ . Polyisobutenes have also excellent resistance to weathering and ultraviolet light [1]. Nevertheless, polyisobutene materials exhibit poor mechanical properties due to creeping and low resistance to penetration. These materials are not resistant to organic solvents (benzene, toluene or petroleum ethers) and to solvent containing materials such as lacquers, fats and oils.

In order to improve the mechanical properties of polyisobutenes, and overcome other PIB weaknesses, like creeping and poor resistance to organic solvents without impairing their low permeability to gas, the syntheses of polyisobutene combinations with polymers displaying good mechanical properties are investigated. Such combinations of PIB with thermoplastic polymers must be stable over time and can be

\* Corresponding author. Tel.: +33 13 42 57 050; fax: +33 13 42 57 070.  
E-mail address: [dominique.teyssie@chim.u-cergy.fr](mailto:dominique.teyssie@chim.u-cergy.fr) (D. Teyssié).

achieved by blending or copolymer elaboration. For example, Storey et al. synthesized a series of linear and three-arm star poly(styrene-*b*-isobutene-*b*-styrene) (PS-PIB-PS) block copolymers with various block compositions via living carbocationic polymerization [2]. From these block copolymers, ionomer block copolymer have been obtained by PS block sulfonation. After sulfonation, physical cross-linking remains stable at temperature higher than the  $T_g$  of PS and the introduction of 5–20 mol% of sulfonate groups into the PS phases has increased tensile modulus and strength [3,4].

Another and single possibility to obtain a thermoplastic reinforced elastomer is to combine both polymers inside an interpenetrating polymer network (IPN) architecture which is defined as the combination of two or more polymer networks synthesized in juxtaposition [5,6]. The entanglement of two cross-linked polymers leads to forced ‘miscibility’ compared with usual blends and the resulting materials exhibit a good dimensional stability. These types of polymer associations in general lead to materials with better mechanical properties, increased resistance to degradation and a possibly synergistic combination of the properties of their components. The semi-IPNs differ from IPNs in that they are composed of a non-cross-linked polymer entrapped in another polymer network and unable to reptate out. IPNs can be prepared through different synthetic routes among which the in situ technique usually proves to be the most convenient technique described in the literature [5,6]. All reactants being present in the starting reaction medium, the reactions leading to the formation of networks can be initiated at the same time leading either to the simultaneous formation of the networks or to a more or less sequential one depending on the experimental conditions. Hence, the reaction mechanisms leading to both network partners must be of different nature, otherwise a single copolymer network is formed.

Introduction of PIB into such a structure is only possible from telechelic polyisobutylene oligomers whose synthesis has been recently developed. For example, the synthesis and characterizations of PIB/polydimethylsiloxane bicomponent networks in which PDMS chains have been cross-linked through allyl-trifunctional polyisobutene via a hydrosilylation reaction have been reported [7–9]. Bicomponent new nanostructured conetworks of poly(ethyl acrylate)-linked-polyisobutene have been synthesized from copolymerization of  $\alpha,\omega$ -dimethacrylic PIB and ethylacrylate on one hand [10] and poly(ethyleneoxide)-linked-polyisobutene conetworks prepared from condensation of hydroxy-telechelic three-arm star PIB with isocyanate telechelic polyethyleneglycol on the other hand [11]. Finally, a new class of amphiphilic polyelectrolyte conetworks composed of hydrophobic polyisobutene and hydrophilic poly(methacrylic acid) segments has been prepared in a broad range of composition [12].

In all above cases, the materials are conetworks.

On the other hand, the synthesis of PIB/polystyrene semi-IPN in which polystyrene is linear has also been reported [13]. Cross-linked networks of butyl rubber (polyisobutylene with 2 mol% isoprene unit) were swollen with various amounts of styrene containing a radical initiator. Polymerization of styrene

inside the PIB network gave elastomeric composites whose mechanical properties depend on polystyrene content.

Generally, little attention is paid to the study of the effect of the relative formation order of both individual networks inside the IPN. However, the network interpenetration degree is highly dependent upon the particular polymer pair that is considered and the best result is sometimes obtained through simultaneous formation of both networks or sometimes through sequential formation [6,14,15]. Simultaneous and sequential in situ strategies are thus studied in order to examine the degree of interpenetration of the networks obtained in both cases. Some systematic studies showing interrelation between network formation order and microphase structure are reported in the literature and again show that whatever relation can be established is highly dependent on the chosen polymer pair [14–17].

The aim of the present work is to improve the mechanical properties of polyisobutene by combining it into IPN architecture with PS. This involves an in situ process in which all components are first mixed together and the networks are then formed more or less simultaneously or sequentially, as it will be shown, according to different reaction mechanisms. The formation of the networks inside the IPN architecture has been investigated by near FTIR spectroscopy. From this study the IPN synthesis conditions leading to highest reaction function conversion and best network interpenetration degree have been established. In order to examine the extent of network interpenetration, thermomechanical properties of the resulting materials have been studied by dynamic mechanical thermal analysis (DMTA). The effects of PS cross-linking density and its weight proportion on the network interpenetration have been particularly studied. Finally, IPN morphologies were also analyzed at the sample surface by atomic force microscopy (AFM).

## 2. Experimental part

### 2.1. Materials

$\alpha,\omega$ -Dihydroxypolyisobutene ( $M_{SEC} = 4200 \text{ g mol}^{-1}$ ,  $I_p = 1.2$  in THF,  $M_{NMR} = 5400 \text{ g mol}^{-1}$  in  $\text{CDCl}_3$ ) was kindly provided by BASF. Dibutyltindilaurate (DBTDL) (Aldrich), divinylbenzene (DVB) (Aldrich) and Desmodur<sup>®</sup> N3300 (Bayer) (NCO content  $21.8 \pm 0.3\%$  according to the supplier) were used as received. This last compound is described as an isocyanate mixture resulting from the condensation of three to several hexamethylene diisocyanate molecules and mainly composed of mono-, di- and tri-isocyanates with a global functionality higher than two. Thus, mere ‘tri(6-isocyanatohexyl)isocyanurate’ is not a proper description and the compound is referred to as ‘isocyanate cross-linker’ [18]. Benzoyl peroxide (BPO, Jansen) and dicyclohexylperoxydicarbonate (DCPD, groupe Arnaud) were dried under vacuum before use. Styrene (Acros) and toluene (Prolabo) were dried on molecular sieves and distilled just before use. Dichloromethane ( $\text{CH}_2\text{Cl}_2$ , Carlo Erba) was used as received.

## 2.2. Synthesis

### 2.2.1. Single network synthesis

The single PIB networks were synthesized as previously described [19,20]. The single PS networks were synthesized as following: styrene (1 g,  $9.6 \times 10^{-3}$  mol) was mixed with DVB (120  $\mu\text{L}$ ,  $8.5 \times 10^{-4}$  mol, 11% by weight with respect to styrene) and the free-radical initiator BPO (5 mg,  $2.1 \times 10^{-5}$  mol, 0.5% by weight with respect to styrene). The mixture was poured under argon into a mould made from two glass plates clamped together and sealed with a 1 mm thick Teflon<sup>®</sup> gasket. The mould was heated in an oven at 60 °C for 5 h and at 80 °C for 2 h and 100 °C for 2 h. A rigid transparent film was obtained.

### 2.2.2. PIB/PS IPN synthesis

For the PIB/PS (50:50) IPN, 1 g  $\alpha,\omega$ -dihydroxypolyisobutene (0.45 OH mequiv.) was mixed with 1 g styrene ( $9.6 \times 10^{-3}$  mol) and 120  $\mu\text{L}$  DVB ( $8.5 \times 10^{-4}$  mol, 11% by weight with respect to styrene) under argon. Then, 5 mg BPO ( $2.1 \times 10^{-5}$  mol, 0.5% by weight with respect to styrene), 0.13 g Desmodur<sup>®</sup> N3300 (0.68 NCO mequiv.,  $[\text{NCO}]/[\text{OH}] = 1.5$ ) and 3  $\mu\text{L}$  DBTDL ( $5.9 \times 10^{-6}$  mol,  $[\text{DBTDL}]/[\text{OH}] = 0.013$ ) were added. The mixture was degassed and then poured under argon into a mould as described previously. The mould was heated in an oven at 60 °C for 5 h, at 80 °C for 2 h and up to 100 °C for 2 h.

IPNs with different PS contents ranging from 20 to 90% by weight were synthesized keeping the same relative proportions between monomer, cross-linker and catalyst or initiator for each network. So, an IPN obtained from a mixture of 0.70 g  $\alpha,\omega$ -dihydroxypolyisobutene and 0.30 g styrene will be noted PIB/PS (70:30) IPN.

## 2.3. Analytical techniques

In order to estimate the amount of uncrosslinked starting materials in the final product and thus the extent of network formation, single networks and IPNs were extracted in a Soxhlet with dichloromethane for 72 h. After extraction, the sample was dried under vacuum and then weighed. The extracted content (EC) is given as a weight percentage:

$$\text{EC}(\%) = \frac{(W_0 - W_E)}{W_0} \times 100$$

where  $W_0$  and  $W_E$  are the weights of samples before and after extraction, respectively.

The extracted materials, when significant amount thereof, were analyzed by <sup>1</sup>H NMR spectroscopy.

### 2.3.1. FTIR spectroscopy

The rates of the network formation in the  $\alpha,\omega$ -dihydroxypolyisobutene/styrene (20:80) (wt/wt) mixture were followed in the bulk and in real time in the infrared region (7500–1800  $\text{cm}^{-1}$ ). The PS network formation as well as that of the urethane bonds were followed by monitoring the disappearance

of characteristic absorption bands of the C=C–H vinyl bond at 6136  $\text{cm}^{-1}$  and of the isocyanate function at 2270  $\text{cm}^{-1}$ , respectively, as described previously [21]. A given peak area is directly proportional to the reagent concentration (the Beer–Lambert law has been checked for both absorption bands with the  $\alpha,\omega$ -dihydroxypolyisobutene/styrene (20:80) (wt/wt) mixture and a 250  $\mu\text{m}$  thick Teflon<sup>®</sup> gasket), thus the conversion-time profile can be easily derived from the spectra recorded as a function of time. The conversion of reactive bonds can be calculated as  $p = 1 - (A_t/A_0)$  from the absorbance values where the symbols have the usual meaning and the subscripts 0 and  $t$  denote reaction times.

IPNs were directly synthesized in the IR cell which is made from two calcium fluoride plates separated by a 250  $\mu\text{m}$  thick Teflon<sup>®</sup> gasket. The IR cell was inserted in an electrical heating jacket with an automatic temperature controller (Graseby Specac). The temperature of the cell holder was constant within  $\pm 1$  °C of the set temperature. The infrared spectra were recorded with a Bruker spectrometer (Equinox 55) in the range 7000–1800  $\text{cm}^{-1}$  by averaging 10 consecutive scans with a resolution of 4  $\text{cm}^{-1}$ . Scan accumulations were repeated every 10 min during the kinetic measurements.

### 2.3.2. Dynamic mechanical analysis

Dynamic mechanical thermal analysis (DMTA) measurements were carried out on film samples with a Q800 apparatus (TA Instruments) operating in tension mode. Experiments were performed at a 1 Hz frequency and a heating rate of 3 °C  $\text{min}^{-1}$  from –100 to 200 °C. Typical dimensions of the samples were 30 mm  $\times$  8 mm  $\times$  0.5 mm. The set up provides the storage and loss modulus ( $E'$  and  $E''$ ) and the damping parameter or loss factor ( $\tan \delta$ ). All storage modulus values were normalized at 3 GPa at –100 °C in order to compare their relative evolution with increasing temperature.

The stress–strain experiments were carried out with the same size samples on the same apparatus with a deformation rate of 1 mm  $\text{min}^{-1}$  at 35 °C. At least four measurements for each sample are carried out and a representative stress–strain curve is reported.

### 2.3.3. Material ageing

The material ageing study was performed by UV exposure (500 W) at 35 °C (Helios Italquartz). The absorbances of single networks and IPNs were measured with a Jasco V570 spectrometer at 350 nm every 24 h and the absorbance variation ( $\Delta A$ ) was calculated as

$$\Delta A = \frac{A_t - A_0}{A_0}$$

where  $A_0$  and  $A_t$  are the sample absorbance before and after UV exposure, respectively.

### 2.3.4. Atomic force microscopy

The atomic force microscopy (AFM) apparatus was composed of a Dimension 3100 Scanning Probe Microscope and a NanoScope<sup>®</sup> IIIa from VEECO working at 22 °C.

The scanning window can vary from 100  $\mu\text{m}$  down to a few nanometers. The probe tip frequency resonance was  $f_0 = 250$  kHz.

### 3. Results and discussion

The thermomechanical properties of polyisobutene (PIB) elastomers must be improved in order to make it suitable for new applications [22]. In a first step, we had first tried to improve its mechanical properties by combining a PIB network with a polymethylmethacrylate (PMMA) one into an interpenetrating polymer network (IPN) architecture [19]. Nevertheless, in this case the different network precursors are not miscible and toluene must be added as a solvent, which is not desirable for further practical applications. For this reason, we now focused our attention on another partner for PIB, i.e. polystyrene (PS). Indeed, styrene is both the PS network precursor and a good solvent for the telechelic PIB oligomer used here, so that, no solvent is necessary for these PIB/PS IPN syntheses.

All the IPNs have been synthesized according to the in situ method, i.e. all the starting products are mixed together, i.e. monomer, oligomer, cross-linkers, catalyst and initiator to give a homogeneous solution. Polystyrene network is prepared by free-radical copolymerization of styrene with divinylbenzene (DVB) as the cross-linking agent and BPO as the initiator. The PIB network is cross-linked through its OH end groups with the pluri-isocyanate cross-linker. The alcohol/isocyanate reaction is catalyzed by DBTDL leading to urethane cross-links.

The network interpenetration degree is highly dependent upon the particular polymer pair which is considered, and the best result is sometimes obtained through simultaneous formation of both networks or sometimes through sequential formation, i.e. one after the other [6,14,15]. Accordingly, the PIB and PS network formations were studied in order to establish the synthesis conditions leading to the best interpenetration degree of both networks, as well as to a close to quantitative conversion for each precursor.

The styrene polymerization/cross-linking is followed by monitoring the disappearance of the absorption band at  $6130\text{ cm}^{-1}$  [23] the molar extinction coefficient of which is low ( $\epsilon = 0.09\text{ L mol}^{-1}\text{ cm}^{-1}$ ). The PIB network formation is studied through the disappearance of the absorption band of isocyanate groups of the cross-linking agent at  $2270\text{ cm}^{-1}$  [24,25]. All kinetic studies described below are performed on  $\alpha,\omega$ -dihydroxypolyisobutene/styrene (20:80) (wt/wt) mixtures leading to a 250  $\mu\text{m}$  thick sample. Under these conditions, the two absorption bands follow the Beer–Lambert law and can be recorded as a function of time simultaneously on the same sample. The conversion versus time curves is calculated from these measurements. In order to determine the PIB hydroxyl group conversion during the cross-linking, it must be assumed here that each NCO group which disappears reacts only with one PIB OH group (although some uncertainty remains whether a NCO group can be destroyed by contaminating water for instance). The PIB networks are synthesized at  $60^\circ\text{C}$  in order to minimize the occurrence of side-reactions such as

biuret and isocyanurate formations which are favored at high temperature [18,26].

#### 3.1. Respective rates of PIB and PS network formation inside the IPN

##### 3.1.1. PIB network formation

**3.1.1.1. Influence of cross-linker concentration.** In a first step, the PIB network formation is examined in the presence of the second network precursors (styrene, divinylbenzene and BPO) by FTIR spectroscopy. The isocyanate cross-linker and catalyst (DBTDL) amounts are varied in order to obtain the maximum OH group conversion. The parameter  $r$  is defined as the ratio of the initial NCO to OH concentrations ( $r = [\text{NCO}]_0/[\text{OH}]_0$ ). These molar ratios are calculated from PIB oligomer molecular weight measured from  $^1\text{H}$  NMR and from NCO content  $21.8\% \pm 0.3\%$  indicated by the supplier. However, the PIB oligomer molecular weight has been determined both by SEC ( $M_n = 4200\text{ g mol}^{-1}$ ) and  $^1\text{H}$  NMR ( $M_n = 5400\text{ g mol}^{-1}$ ). The  $[\text{NCO}]/[\text{OH}]$  ratio goes down to 1.18 if the SEC molecular weight is taken into account instead of 1.50 if the NMR  $M_n$  is chosen. However, it was checked that similar kinetic results are obtained in both cases and the  $^1\text{H}$  NMR value will be taken into account. The hydroxyl group conversion is deduced from the isocyanate conversion and  $r$  assuming that each isocyanate group reacts with one hydroxyl group without any side-reaction. The first chosen  $[\text{DBTDL}]/[\text{OH}]$  molar ratio is equal to 0.013. BPO and DVB are introduced at 0.5 and 11% by weight with respect to styrene, respectively. Each mixture is cured at  $60^\circ\text{C}$  for 3 h. Under those conditions, the styrene characteristic absorption band does not vary throughout the PIB network formation showing that styrene just behaves as an inert solvent.

The OH conversion–time curves have the same shape for all  $r$  values varying from 0.77 to 2.00 as shown in Fig. 1. The OH conversion increases until a pseudo-plateau the position of which increases from 0.40 to 0.90 when  $r$  varies from 0.77 to 2.00. When  $r$  increases from 0.77 to 1.50 the OH conversion at 180 min increases from 0.49 to 0.83. When  $r$  is higher than 1.5,

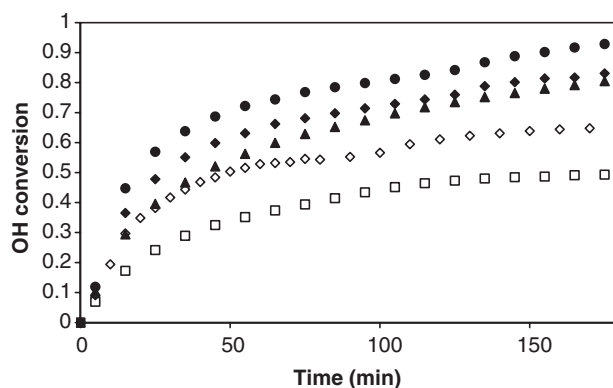


Fig. 1. Hydroxyl conversion versus time for different  $r$  values (□) 0.77, (◇) 1.00, (▲) 1.28, (◆) 1.50 and (●) 2.00— $\alpha,\omega$ -dihydroxypolyisobutene/styrene (20:80) (wt/wt)—0.5% BPO and 11% DVB by weight with respect to styrene— $[\text{DBTDL}]/[\text{OH}] = 0.013$ — $T = 60^\circ\text{C}$ .

the OH conversion after 180 min does not exceed 0.90: the large NCO excess does not help increasing the OH conversion at 60 °C. This NCO excess requirement probably arises both from the high viscosity and low mobility of the PIB oligomer and the isocyanate cross-linker but it is not necessary to introduce a  $[NCO]/[OH]$  molar ratio higher than 1.5. As shown in a next part, the hydroxyl conversion reaches 100% when the temperature is increased for the IPN formation.

In all IPN synthesis,  $r$  will be set to 1.5 in order to ensure a maximum hydroxyl function conversion rate without introducing a too large isocyanate function excess in the medium that could promote side-reactions.

From those conversion–time curves, the kinetic order of the alcohol–isocyanate addition could be determined according to the following equation:

$$\frac{-d[OH]}{dt} = \frac{-d[NCO]}{dt} = k[NCO]^\alpha [OH]^\beta \quad (1)$$

where  $k$  is the apparent rate constant and  $\alpha$  and  $\beta$  the partial orders with respect to NCO and OH groups, respectively. The global order  $\alpha + \beta$  can be determined from the hydroxyl conversion–time curve recorded for  $r = 1$ , since Eq. (1) becomes:

$$\frac{-d[OH]}{dt} = k[OH]^{\alpha+\beta} \quad (2)$$

In solution, the alcohol–isocyanate addition reaction follows a first order kinetics with respect to each reactive group [26,27]. Since, the PIB network is synthesized in presence of styrene which does not react in the chosen conditions, the alcohol–isocyanate addition leading to PIB network formation occurs in solution and the kinetic orders may be equal to one with respect to each reactive function, thus  $\alpha + \beta = 2$ . The Eq. (2) becomes:

$$\frac{1}{[OH]_t} - \frac{1}{[OH]_0} = kt \quad (3)$$

where  $[OH]$  are the alcohol concentration and the subscripts 0 and  $t$  denoting reaction times.

Eq. (3) may be written introducing the OH conversion ( $p$ ) as

$$\frac{p}{1-p} = kt[OH]_0$$

with

$$p = \frac{[OH]_0 - [OH]_t}{[OH]_0} \quad (4)$$

The  $p/1-p$  linear dependence with time is verified for the first 30 min of reaction ( $p/1-p = 0.026 \times t$  (linear regression coefficient: 0.993) when  $r = 1$ ), thus the isocyanate–alcohol addition obeys second order kinetics in the synthesis conditions of the PIB network.

When  $r$  is different from 1, Eq. (1) is integrated with the same assumption that  $\alpha$  and  $\beta$  are equal to 1 and becomes:

$$\frac{1}{[OH]_0 - [NCO]_0} \ln \left( \frac{[NCO]_0 \times [OH]_t}{[OH]_0 \times [NCO]_t} \right) = kt \quad (5)$$

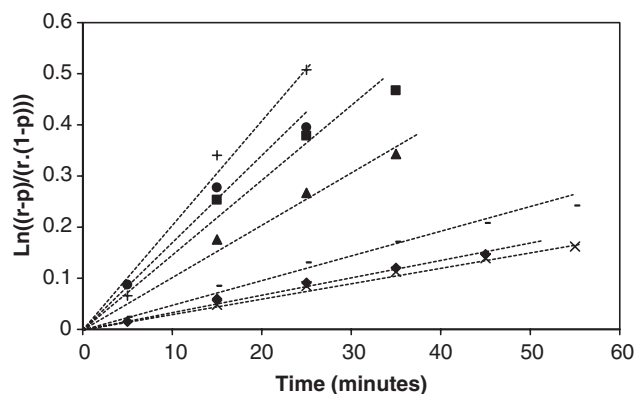


Fig. 2. Second order kinetics for hydroxyl end chain of the PIB with the isocyanate cross-linker for different  $[NCO]/[OH]$  molar ratios, (◆) 1.14, (×) 1.17, (–) 1.27, (▲) 1.50, (■) 1.65, (●) 1.78 and (+) 2.00— $\alpha,\omega$ -dihydroxypolyisobutene/styrene (20:80) (wt/wt)—0.5% BPO and 11% DVB by weight with respect to styrene— $[DBTDL]/[OH] = 0.013$ — $T = 60$  °C.

or

$$\ln \left( \frac{r-p}{r(1-p)} \right) = k[OH]_0(r-1)t \quad (6)$$

Fig. 2 displays the  $\ln((r-p)/(r(1-p)))$  versus time curves for each  $r$  value above 1. A linear variation is always observed, thus the partial kinetic orders are equal to 1 with respect to each reactive group, in agreement with the values in the literature for the isocyanate–alcohol addition in solution [24]. Thus, the cross-linking reaction kinetics remains similar to the related solution kinetics while being carried out in the presence of the second network precursor.

**3.1.1.2. Influence of catalyst concentration.** Then, the catalyst amount of the isocyanate–alcohol addition is also optimized in order to obtain a fast PIB network formation and a maximum OH function conversion. PIB networks are synthesized with different  $[DBTDL]/[OH]$  molar ratios varying from 0 to 0.13 for  $\alpha,\omega$ -dihydroxypolyisobutene/styrene (20:80) (wt/wt) mixtures containing 11% DVB and 0.5% POB by weight with respect to styrene. The  $r$  value and temperature are set at 1.5 and 60 °C, respectively. Under those conditions, the characteristic C=C absorption band of styrene remains unchanged, i.e. styrene does not react and should be considered just as an inert solvent.

The OH conversion–time curves are reported in Fig. 3(A). Without the tin-based-catalyst the reactivity of the OH groups of the PIB oligomer is very low: the hydroxyl conversion reaches only 0.24 in 180 min at 60 °C. In the presence of DBTDL, all conversion curves exhibit the same shape and reach a plateau the position of which depends on the  $[DBTDL]/[OH]$  ratio: the higher the catalyst concentration, the higher the initial reaction rate and the OH conversion at 180 min as shown in Fig. 3(B). The OH conversion at 180 min increases from 0.24 to 0.87 when the  $[DBTDL]/[OH]$  molar ratio increases from 0 to 0.013 and then tends to an asymptotic value of one on increasing the  $[DBTDL]/[OH]$  up to 0.013. When the  $[DBTDL]/[OH]$  molar ratio is above 0.013 the conversion at

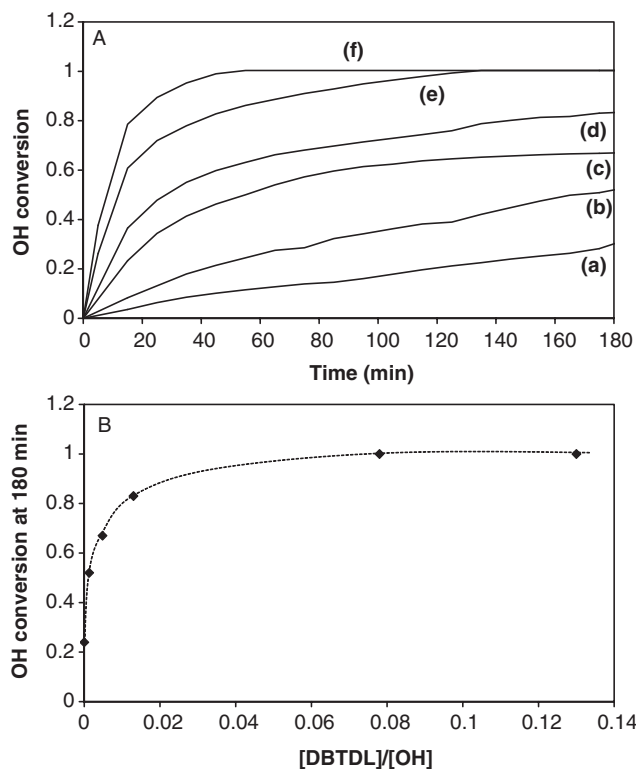


Fig. 3. (A) OH conversion versus time with different [DBTDL]/[OH] ratios (a) 0, (b) 0.001, (c) 0.005, (d) 0.013, (e) 0.078 and (f) 0.130. (B) OH conversion at 180 min versus [DBTDL]/[OH] molar ratio— $\alpha,\omega$ -dihydroxypolyisobutene/styrene (20:80) (wt/wt)—0.5% BPO and 11% DVB by weight with respect to styrene—[NCO]/[OH]=1.5— $T=60^\circ\text{C}$ .

the plateau still increases slightly but a new absorption peak characteristic of biuret and isocyanurate groups appears at  $2336\text{ cm}^{-1}$ . In order to avoid these side-reactions, the [DBTDL]/[OH] molar ratio is set to 0.013 for all next studies.

The values of apparent rate constant  $k$  of the isocyanate–alcohol addition leading to the PIB network formation and defined in Eq. (1) could be determined from the previous experiments.  $k$  is decomposed as follows [28]:

$$k = k_0 + k_{\text{cat}}[\text{DBTDL}] \quad (7)$$

where  $k_0$  and  $k_{\text{cat}}$  are spontaneous and catalyst kinetic rate constants, respectively. The  $\text{Ln}((r-p)/(r(1-p)))$ -time curves characterizing a second order kinetics are straight lines up to 50% conversion whatever the catalyst concentration. A deviation is observed from second order kinetics for conversions higher than 0.60. A similar behavior has been observed by Deschères et al. [29] concerning the reaction of propyl and phenyl isocyanates with dihydroxy telechelic polybutadienes, and has been explained as urethane group autocatalysis. Knowing the hydroxyl initial concentration ( $[\text{OH}]_0 = 0.073\text{ mol L}^{-1}$ ) and  $r = 1.5$ ,  $k$  is calculated from the slope of the previous curves. Then, in order to determine the spontaneous  $k_0$  and catalyzed  $k_{\text{cat}}$  rate constants, the  $k$  values are reported versus DBTDL concentration (Fig. 4).  $k$  varies linearly with DBTDL concentration lower than  $1 \times 10^{-3}\text{ mol L}^{-1}$  and then raises to a limit when DBTDL concentration is higher. This phenomenon has been already

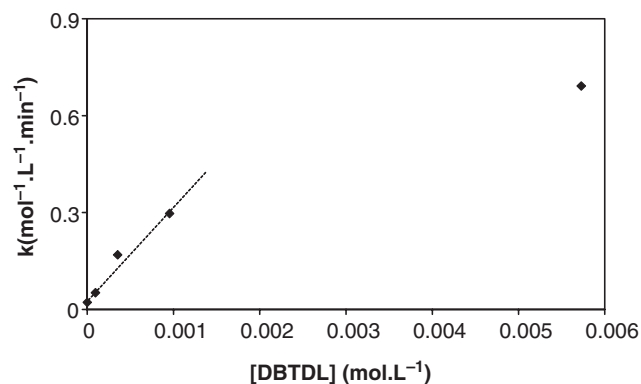


Fig. 4. Apparent kinetic constant  $k$  versus DBTDL concentration— $\alpha,\omega$ -dihydroxypolyisobutene/styrene (20:80) (wt/wt)—0.5% BPO and 11% DVB by weight with respect to styrene—[NCO]/[OH]=1.5— $T=60^\circ\text{C}$ .

observed and is due to the formation of complexes or aggregates [30,31]. Nevertheless, linear dependence is verified again when catalyst aggregation is prevented, i.e. at low concentrations.

According to Eq. (7) and from the linear part of the previous curve, the  $k_0$  and  $k_{\text{cat}}$  rate constants are equal to  $34 \times 10^{-3}$  and  $287\text{ mol}^{-2}\text{ L}^2\text{ min}^{-1}$ , respectively, comparable to those reported in the literature [24]. For example,  $k_0$  and  $k_{\text{cat}}$  are equal to  $2.8 \times 10^{-3}$  and  $190\text{ mol}^{-2}\text{ kg}^{-2}\text{ min}^{-1}$ , respectively, at  $40^\circ\text{C}$  for isocyanato propyl triethoxysilane addition in bulk on hydroxytelechelic polybutadiene.

**3.1.1.3. Influence of temperature.** Finally, in order to determine the thermodynamic parameters of the cross-linking reaction, the temperature effect is studied at 25, 40, 50 and  $60^\circ\text{C}$  always with  $\alpha,\omega$ -dihydroxypolyisobutene/styrene (20:80) (wt/wt) mixtures containing DVB and BPO. The second order kinetics is checked for OH conversion below 0.50 whatever the temperature and  $k$  is measured at each temperature. Thermodynamic parameters are determined using the Arrhenius law (Fig. 5). The pre-exponential factor and activation energy corresponding to the apparent rate constant  $k$  are equal to  $1.1 \times 10^5\text{ min}^{-1}$  and  $36\text{ kJ mol}^{-1}$ , respectively. These results are in agreement with those obtained on addition of polybutadiene with propyl

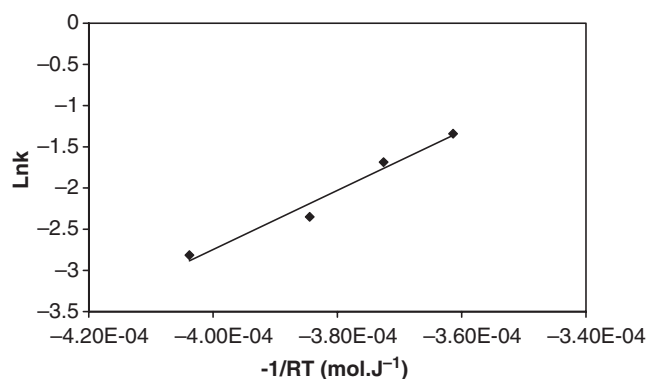


Fig. 5. Second order kinetics. Arrhenius plot for  $\alpha,\omega$ -dihydroxypolyisobutene/styrene (20:80) (wt/wt)—0.5% BPO and 11% DVB by weight with respect to styrene—[NCO]/[OH]=1.5—[DBTDL]/[OH]=0.013—[DBTDL]= $9.54 \times 10^{-5}\text{ mol L}^{-1}$ .

isocyanate ( $E_0=20\text{ kJ mol}^{-1}$ ) [29], phenyl isocyanate ( $E_0=37\text{ kJ mol}^{-1}$ ) [29], isocyanatopropyl triethoxysilane ( $E_0=53\text{ kJ mol}^{-1}$  and  $E_{\text{cat}}=72\text{ kJ mol}^{-1}$ ) [24] or 3-isopropenyl- $\alpha,\alpha$ -dimethyl benzyl isocyanate ( $E_0=61\text{ kJ mol}^{-1}$  and  $E_{\text{cat}}=41\text{ kJ mol}^{-1}$ ) [28] where  $E_0$  and  $E_{\text{cat}}$  are measured without or with catalyst, respectively.

These kinetic studies show that the maximum OH end group conversion of the PIB oligomer is obtained at  $60\text{ }^\circ\text{C}$  with [DBTDL]/[OH] and [NCO]/[OH] molar ratios equal to 0.013 and 1.5, respectively. These values are accordingly kept for all further experiments. Under these conditions, the PIB network is synthesized in presence of the second network precursors (styrene, DVB and BPO). The cross-linking or/and the different precursor presence do not affect the kinetics of alcohol–isocyanate addition. Indeed, apparent kinetic constant, activation energy and pre-exponential factor calculated from the FTIR measurements are in agreement with those reported for simple chain end modification by similar reactions.

### 3.1.2. PS network formation

The formation of the polystyrene (PS) network in the presence of PIB network is in a next step also examined by FTIR spectroscopy. The PS network synthesis is performed at  $60\text{ }^\circ\text{C}$  with different radical initiator BPO amounts varying from 0.5 to 5% by weight with respect to styrene. In a first step, we have checked that PIB network formation is hardly affected by the BPO amount. On the other hand, as expected, the initial vinyl conversion rate increases with the BPO amount as shown in Fig. 6(A). Thus, the conversion reaches about 7 and 60% at 300 min with 0.5 and 5% BPO by weight with respect to styrene, respectively.

The effect of the PIB network presence on the PS network formation is studied in the first stage of the free-radical polymerization. The linearity of  $\text{Ln}([M]_0/[M])$  versus time gives evidence that the internal order of the reactions with respect to styrene is equal to one (Fig. 6(A)). The apparent rate constant ( $k_{\text{app}}$ ) value for the copolymerization process of styrene with divinylbenzene at  $60\text{ }^\circ\text{C}$  inside PIB network is determined from the slope of the plots (Table 1).

Contrary to the classical free-radical polymerization in solution or in bulk,  $k_{\text{app}}$  is not found proportional to square root of the initiator concentration. In order to check if this non-linearity is due to PIB network presence, PS network formation kinetic has been studied with DCPD as the initiator. Indeed, its decomposition at  $60\text{ }^\circ\text{C}$  is faster (half-life time at  $60\text{ }^\circ\text{C}\approx 54\text{ min}$  [27]) than that of BPO (half-life time at  $60\text{ }^\circ\text{C}=45\text{ h}$  [27]) and the PS network is formed before PIB one as shown in Fig. 6(B). The linearity of  $\text{Ln}([M]_0/[M])$  versus time still gives evidence that the internal order of the reaction with respect to styrene is equal to one (Fig. 6(B)).  $k_{\text{app}}$  values measured from these curves (Table 1) are proportional to the square root of the DCPD concentration but the straight line does not go through the origin. The DCPD decomposition is very fast at  $60\text{ }^\circ\text{C}$  and the quasi-stationary state approximation might not be valid under those conditions.

The PS network formation kinetics with BPO and DCPD at  $60\text{ }^\circ\text{C}$ , i.e. in the presence or not of the PIB network, shows that

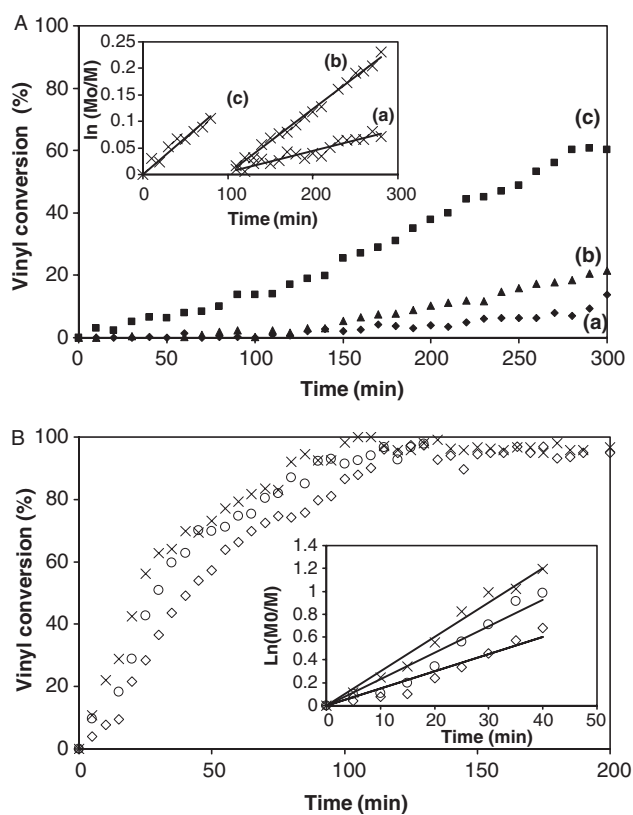


Fig. 6. Vinyl conversion versus time with different (A) BPO content (a) 0.5, (b) 1 and (c) 5% and (B) DCPD content ( $\times$ ), ( $\circ$ ) 7 and ( $\diamond$ ) 5% by weight with respect to styrene. Insert figure:  $\text{Ln}([M]_0/[M])$  versus time curves— $\alpha,\omega$ -dihydroxypolyisobutene/styrene (20:80) (wt/wt)—11% DVB by weight with respect to styrene—[NCO]/[OH]=1.5—[DBTDL]/[OH]=0.013— $T=60\text{ }^\circ\text{C}$ .

the PS network formation kinetic is indeed affected by the presence of the PIB network. Unusual polymerization kinetic behaviors have already been observed in the IPN in situ synthesis and have been correlated with the changes of viscosity and morphology of the systems [32].

### 3.1.3. PIB and PS network formation order

Different authors have reported that the first formed network induces and determines the morphology and properties of the final material [5,6]. In order to check such synthesis effects on the morphology and the interpenetration of the networks, the experimental conditions in which the synthesis of the networks will be simultaneous or sequential are now systematically

Table 1

$k_{\text{app}}$  calculated from the slope of  $\text{Ln}([m]_0/[m])$  versus time curves for styrene vinyl group conversion below 10%— $\alpha,\omega$ -dihydroxypolyisobutene/styrene (20:80) (wt/wt) mixture—11% DVB by weight with respect to styrene—[NCO]/[OH]=1.5—[DBTDL]/[OH]=0.013— $T: 60\text{ }^\circ\text{C}$

Initiator	Weight content (%)	Initiator ( $\text{mol L}^{-1}$ )	$k_{\text{app}}$ ( $\text{min}^{-1}$ )
BPO	0.5	0.002	0.001
BPO	1	0.003	0.012
BPO	5	0.016	0.014
DCPD	5	0.014	0.015
DCPD	7	0.019	0.023
DCPD	10	0.028	0.030

examined. The alcohol–isocyanate addition cannot be inhibited at 60 °C thus the network formation order can only be modified by the speeding up or slowing down rate of the PS network synthesis. Thus, the initiator nature (BPO or DCPD) and its amount varying from 0.5 to 5% by weight with the respect to styrene have been systematically varied. In order to obtain a quantitative conversion of the hydroxyl and vinyl groups, after 300 min at 60 °C, the temperature is raised up to 80 °C for 120 min and then to 100 °C for 120 min.

First, in order that the PS network be synthesized after the PIB one is achieved, 0.5% BPO by weight with respect to styrene is introduced in the initial mixture. Vinyl and hydroxyl conversion versus time curves are shown in Fig. 7. The hydroxyl conversion rate is fast for the first 40 min at 60 °C. Then the OH conversion increases from 40 to 90% for the next 260 min at 60 °C and still increases from 90 to 100% when the temperature is increased to 80 °C. A quantitative conversion of the OH groups is obtained under those synthesis conditions, without any side reaction probably because of the low isocyanate amount remaining at this stage of the reaction.

As expected, the vinyl conversion is low at 60 °C (the conversion reaches about 7% after 300 min), due to a weak decomposition of BPO at 60 °C (half-life time at 60 °C = 45 h [27]). Then the temperature is increased to 80 °C for 120 min and the vinyl conversion increases rapidly from 7 to 75%. Then, a post-cure is carried out at 100 °C for 120 min and the vinyl conversion increases from 75 to 85%.

In this way, the network formations are sequential when the BPO concentration is equal to 0.5% by weight with respect to styrene. Preferentially, the isocyanate/hydroxyl addition reaction allowing the PIB network formation is carried out at 60 °C for 300 min. At this temperature, the styrene polymerization and cross-linking reactions slightly occur. The PS network synthesis further proceeds when the temperature is increased to 80 °C. A higher final conversion is reached when a post-cure is carried out at 100 °C for 2 h.

In order to speed up the PS network formation a 5% BPO amount (instead 0.5% with respect to styrene) is introduced in

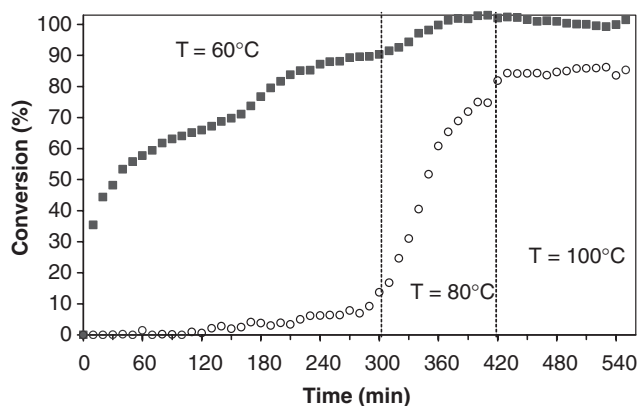


Fig. 7. (■) OH and (○) CH<sub>2</sub>=CH- conversion versus time— $\alpha,\omega$ -dihydroxypolyisobutene/styrene (20:80) (wt/wt) mixture—0.5% BPO and 11% DVB by weight with respect to styrene—[NCO]/[OH]=1.5—[DBTDL]/[OH]=0.013—60 °C for 300 min, 80 °C for 120 min, then 100 °C for 120 min.

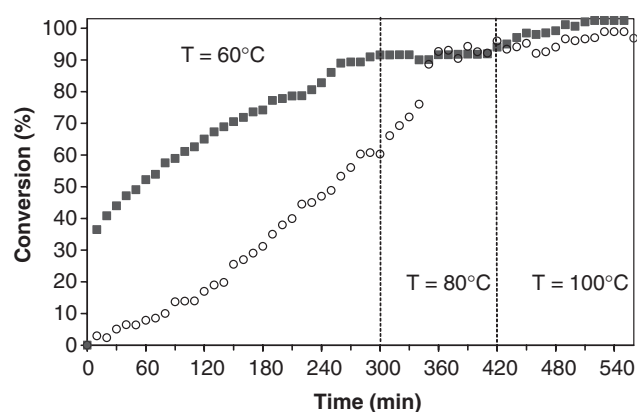


Fig. 8. (■) OH and (○) CH<sub>2</sub>=CH- conversion-time curves— $\alpha,\omega$ -dihydroxypolyisobutene/styrene (20:80) (wt/wt) mixture—5% BPO and 11% DVB by weight with respect to styrene—[NCO]/[OH]=1.5—[DBTDL]/[OH]=0.013—60 °C for 300 min, 80 °C for 120 min, then 100 °C for 120 min.

the reactive medium that is then heated at 60 °C. The reactive bond conversions are reported in Fig. 8.

As expected, the hydroxyl conversion is hardly affected by the BPO amount. On the other hand, after 300 min at 60 °C, the vinyl conversion is about 60% (compared with 7% with 0.5% BPO). The styrene conversion increases from 60 to 95% when the temperature is increased to 80 °C for 120 min. Indeed the remaining BPO decomposes quickly at this temperature (half-life time = 3.7 h [27]) and the PS network formation is nearly quantitative. During the post-cure at 100 °C, the conversion does not change dramatically. The final conversion of the vinyl functions is higher, while the synthesis is quasi-simultaneous rather than sequential.

A last possibility is to synthesize the PS network before the PIB one. In a first step, the styrene photopolymerization at room temperature has been considered but a macroscopic phase separation is always observed due to PIB and polystyrene incompatibility ( $\delta_{\text{PIB}} = 18.50$ ,  $\delta_{\text{PS}} = 18.19$  MPa<sup>1/2</sup> at 25 °C [33]). For this reason, a chemical polymerization/cross-linking reaction has been used. Thus, dicyclohexylperoxydicarbonate (DCPD) is chosen as the free-radical initiator because its decomposition is very fast at 60 °C (half-life time at 60 °C = 54 min [27]). The OH and vinyl conversions are shown in Fig. 9.

Both networks are formed simultaneously for the first 30 min. The vinyl conversion reaches 95% after 120 min but the PIB network formation is slower than under the previous conditions and the hydroxyl conversion only reaches 38% after 60 min. This conversion remains unchanged by the temperature increase to 80 °C and the post-cure at 100 °C. This low conversion is explained by the fact that the synthesis occurs below PS glass transition temperature. So, the formed PS network is in its glassy state at the current reaction temperature and hinders the PIB network formation since the PIB chains cannot move in order to react further. This behavior has already been observed during the PMMA/PDMS [15,34] and PIB/PMMA [19] IPN synthesis in which PMMA network is formed first.



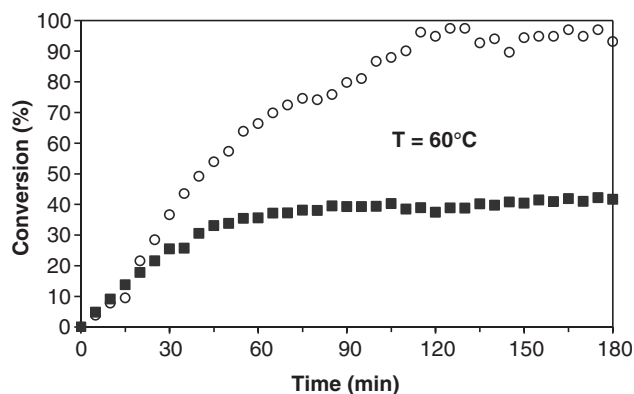


Fig. 9. (■) OH and (○) CH<sub>2</sub>=CH- conversion versus time— $\alpha,\omega$ -dihydroxypolyisobutene/styrene (20:80) (wt/wt) mixture—5% DCPD and 11% DVB by weight with respect to styrene—[NCO]/[OH]=1.5—[DBTDL]/[OH]=0.013— $T=60^\circ\text{C}$ .

The experimental conditions allowing the quasi-simultaneous or sequential synthesis of both networks inside the IPNs have now been established. A quasi-simultaneous synthesis of PIB and PS networks is obtained when a 5% BPO concentration is used as the free-radical initiator. The PS network is formed after the PIB one when just 0.5% BPO is introduced in the medium. In order to build the PS network before the PIB one 5% DCPD concentration was also tentatively used. The first formed network generally induces and determines the morphology and properties of the final material, therefore, the samples synthesized with those different approaches are now characterized.

## 3.2. Characterizations

### 3.2.1. Macroscopic aspect and extractible products

The refractive indices of PIB and PS are 1.50 and 1.57 at 25 °C, respectively, [35]. Due to their difference, an opaque material is characteristic of a phase separation between both networks; and the material transparency witnesses the quality of the degree of interpenetration. Pictures of IPNs synthesized as previously described are shown in Fig. 10 where their transparent or opaque aspect clearly appears.

The final material is white (Fig. 10(c)) which is characteristic of a large phase separation between both polymers when the PS network is formed before the PIB one. Moreover, the same sample extracted in a Soxhlet contains 20% weight of extracted product, an amount which is in agreement with the low hydroxyl conversion measured by

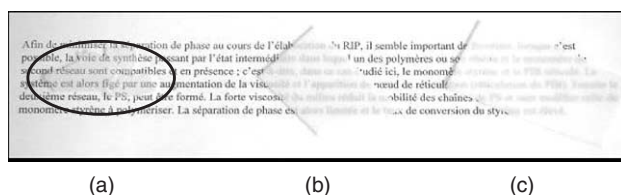


Fig. 10. Picture of different PIB/PS (20:80) IPN obtained from different synthesis conditions: (a) sequential with first PIB (0.5% BPO), (b) quasi-simultaneous (5% BPO) and (c) sequential with first PS (5% DCPD).

FTIR spectroscopy (about 38%—Fig. 9). Analysis of the extracted compounds by <sup>1</sup>H NMR shows that they are mainly composed of extended linear PIB chains. Thus, the PIB network cross-linking cannot be considered as satisfactory, and a macroscopic phase separation occurs.

The PIB/PS (20:80) IPN is translucent (Fig. 10(b)) and shows a turbidity of 3.04 (measured at 460 nm on 0.5 mm thick sample) [6,5] when the network synthesis is quasi-simultaneous (5% BPO) (Fig. 8). The extracted product amounts to 2%. Thus, the phase separation is somewhat limited compared with the previous sample.

Finally, the most transparent PIB/PS (20:80) IPN is obtained when the PIB network is formed before the PS one (0.5% BPO) (Figs. 7 and 10(a)). Indeed, its turbidity value is equal to 0.42 when measured at 460 nm and the extracted product mainly composed of PS linear chains amounts to 1%. The material transparency is directly associated with the polymer domain size: the more transparent the material, the smaller the polymer domain size and the higher the interpenetrating degree of the networks. Thus, the interpenetration between both polymer networks is better when the synthesis is sequential, i.e. when the PIB network is formed before the PS one.

### 3.2.2. Thermal and thermomechanical properties

The viscoelastic behavior of PIB/PS (20:80) IPNs synthesized according to different synthesis pathways has been characterized by DMTA analysis. DSC measurements have also been carried out but no exploitable transition has been detected. Storage modulus ( $E'$ ) versus temperature curves of different PIB/PS (20:80) IPNs are shown in Fig. 11, together with single PIB and PS network thermomechanical properties. PIB network (Fig. 11(e)) shows a  $\alpha$ -relaxation composed of a peak centered at  $-30^\circ\text{C}$ , corresponding to the  $T_{\alpha}$  of PIB and a low temperature shoulder ( $-50^\circ\text{C}$ ) which has been observed in other PIB based materials [3,36]. These two mechanical relaxation temperatures have been associated with the PIB end local rotational chain motion ( $T_{\alpha} = -50^\circ\text{C}$ ) and to the PIB cooperative backbone motion ( $T_{\alpha} = -30^\circ\text{C}$ ) [37–39]. PS network (Fig. 11(a)) shows a  $\alpha$ -relaxation at  $132^\circ\text{C}$ .

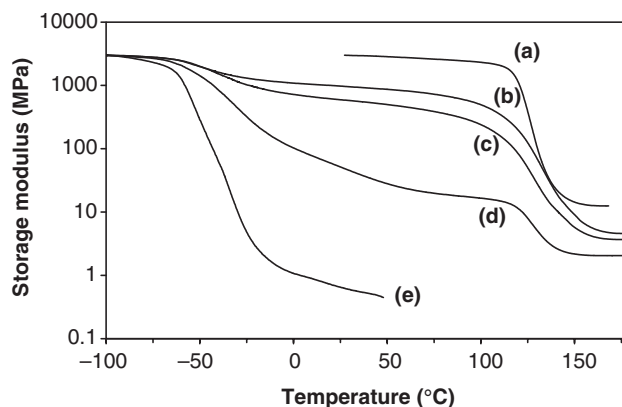


Fig. 11. Storage modulus versus temperature of (a) PS and (e) PIB single networks and PIB/PS (20:80) IPNs in which (b) PIB network is first formed, (c) PIB and PS networks are synthesized quasi-simultaneously and (d) PS network is first formed.

All IPNs show a glassy region below  $-70\text{ }^{\circ}\text{C}$ . Beginning at  $-70\text{ }^{\circ}\text{C}$ , the samples soften and the modulus decreases up to temperatures between  $-30$  and  $0\text{ }^{\circ}\text{C}$ . This storage modulus decrease is associated to PIB rich phase mechanical relaxation. Then, the elastic modulus reaches an intermediate plateau that extends to about  $100\text{ }^{\circ}\text{C}$ , the position of which varies with the synthesis pathway. When the PS network is synthesized before the PIB one (Fig. 11(d)—5% DCPD), the IPN shows the lowest storage modulus (30 MPa at  $50\text{ }^{\circ}\text{C}$ ). The IPN synthesized through a quasi-simultaneous network formation (Fig. 11(c)—5% BPO) has a higher modulus than the previous one (500 MPa at  $50\text{ }^{\circ}\text{C}$ ) but a lower storage modulus than the IPN synthesized by a sequential synthesis pathway wherein the PIB network formation occurs first (860 MPa at  $50\text{ }^{\circ}\text{C}$ ). This last PIB/PS (20:80) IPN which is also the most transparent sample, exhibits the best PS rich phase repartition over the whole materials. Indeed, the storage modulus over the whole range of intermediate temperatures is the highest one, due to the PS rich phase presence over the whole material.

Above  $100\text{ }^{\circ}\text{C}$ , the storage moduli of all IPNs decrease again which is characteristic of the PS rich phase mechanical relaxation. All IPNs possess a dual phase morphology evidenced by two distinct mechanical relaxations beginning respectively at  $-70\text{ }^{\circ}\text{C}$  for the PIB rich phase and  $+100\text{ }^{\circ}$  for the PS rich phase. However, the IPN storage moduli are higher than that of the single PIB network after PIB rich phase mechanical relaxation (0.2 MPa at  $50\text{ }^{\circ}\text{C}$ ). Thus, PIB based material rigidity is clearly improved by the PS network introduction inside these IPN architectures.

In conclusion, the best interpenetrating degree in these IPNs is achieved when PIB network is first synthesized. A PIB network swollen by styrene is thus obtained as an intermediate state. Then the PS network is synthesized inside the PIB network. The PIB network is synthesized in first via an alcohol/isocyanate condensation reaction with [NCO]/[OH] and [DBTDL]/[OH] molar ratios equal to 1.5 and 0.013, respectively, at  $60\text{ }^{\circ}\text{C}$  for 5 h. The PS network is prepared by free-radical polymerization initiated by 0.5% BPO by weight with respect to styrene. This polymerization is released when the temperature is increased to  $80\text{ }^{\circ}\text{C}$ . A post-cure is carried out at  $100\text{ }^{\circ}\text{C}$  for 2 h. Under these conditions, obtained materials are nearly transparent, show low extracted products (1%) and the highest storage modulus at room temperature. These synthesis conditions have been kept for all further studied IPNs.

**3.2.2.1. IPN composition effects.** An improvement of the poor mechanical properties of PIB is thus achieved by combining PIB and PS inside an IPN architecture without the use of a solvent. Accordingly, the IPN composition effect on the material properties has been studied. The IPN samples are synthesized as previously described with different PS weight contents varying from 20 to 90 wt%. The extracted contents of those transparent IPNs are lower than 4% for all PS contents. Their analyses by  $^1\text{H}$  NMR show that they mainly contain PIB.

Storage modulus and  $\tan\delta$  measured versus temperature on those IPNs are shown in Fig. 12. All storage modulus are

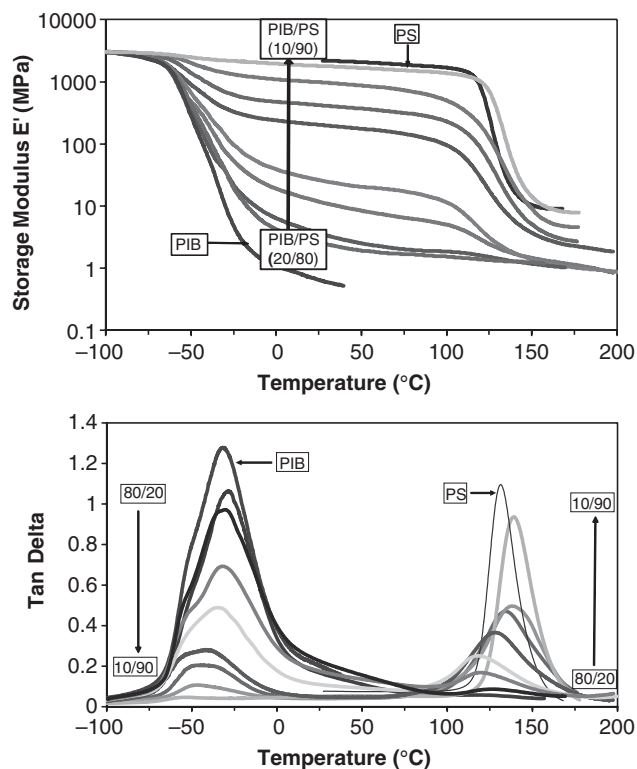


Fig. 12. PS content effect on thermomechanical properties of PIB/PS (100:0, 80:20, 70:30, 60:40, 50:50, 40:60, 30:70, 20:80, 10:90, 0:100) IPNs (A) storage modulus and (B)  $\tan\delta$  versus temperature.

normalized at 3 GPa at  $-100\text{ }^{\circ}\text{C}$  in order to analyze the modulus evolution as a function of PS content. Again, all IPNs show a dual phase morphology evidenced by two distinct mechanical relaxations beginning at  $-70$  and  $+100\text{ }^{\circ}\text{C}$  corresponding to the PIB and the PS rich phases respectively. All samples show a glassy region below  $-70\text{ }^{\circ}\text{C}$ . From  $-70$  to  $0\text{ }^{\circ}\text{C}$ , the samples soften and the modulus decreases dramatically. An intermediate plateau value of the elastic modulus is reached between  $-30$  and  $0\text{ }^{\circ}\text{C}$  and extends to around  $100\text{ }^{\circ}\text{C}$ , which corresponds to the beginning of the PS phase mechanical relaxation. The plateau value increases from 3 to 1800 MPa at  $25\text{ }^{\circ}\text{C}$  when PS weight proportion increases from 20 to 90% (wt) in IPN. Thus, the IPN storage moduli increase with PS weight content, i.e. the PIB network mechanical properties are greatly improved by the PS network introduction.

The  $E'$  versus temperature curves can inform on the degree of interpenetration of phases by studying the slope in the modulus plateau at temperatures between the two mechanical relaxations, i.e. the slope of the rubbery plateau. In immiscible polymer blends, each component retains its identity and exhibits its own  $T_g$ . The resulting modulus temperature curves display two distinct relaxations, each near the  $T_g$  of the respective homopolymers, with a constant modulus plateau between the two. The relative amount of each polymer determines the position, or height, of the plateau, while the flatness of the rubbery plateau is dependent on the degree of phase separation; the more complete the phase separation, the more temperature insensible the modulus becomes [40]. The

slope of this plateau is characteristic of interaction degree between the two phases. In the PIB/PS IPNs, it depends on IPN's composition and varies between  $-3.10^{-3}$  and  $-6.10^{-3}$  MPa K $^{-1}$  with a maximum value for a PIB/PS (50:50) IPN. These values are in agreement with those measured on poly(styrene-*b*-isobutylene-*b*-styrene) block copolymers [3] and suggest that some interactions between the PIB and PS phases inside the PIB/PS IPNs might exist.

Above 150 °C the storage modulus reaches also a plateau depending on the PS content. The plateau value is about 1MPa when PIB is the major component. Then the plateau value increases from 2 to 8 MPa when the PS content increases from 50 to 90% (wt). Materials do not flow at higher temperatures whatever the PS weight proportion and they have a stable modulus until 200 °C. One of our aims is reached here because contrary to TPEs, IPNs do not creep above 150 °C and have a stable modulus higher than a single PIB network whatever PS weight proportion.

The  $\tan \delta$  values are associated with segmental chain motion appearance and are also greatly influenced by the IPN composition. The  $\tan \delta$  peak at  $-30$  °C that corresponds to the PIB rich phase mechanical relaxation decreases when the PS amount increases. Simultaneously, the  $\tan \delta$  peak located around 140 °C corresponding to the PS rich phase increases and becomes narrower.

For IPNs mainly composed of PIB, the PS rich phase mechanical relaxation is located at a lower temperature than that of the single PS network. PIB chains could act as a plasticizer into the PS rich phase, shifting the mechanical relaxation of the PS rich phase. On the other hand, when the PS weight content is higher than 60% this peak is observed at a higher temperature ( $T_{\alpha} = 140$  °C for PIB/PS (20:80) IPN) than that of the PS single network ( $T_{\alpha} = 132$  °C). The same phenomenon has been reported for PDMS/PMMA IPNs and is explained by a local increase of PMMA phase cross-linking density [41,42]. In addition to these observations, the  $\tan \delta$  shift versus temperature has been measured in the case of PIB/PS semi-IPNs, i.e. in which the PS is uncross-linked (Fig. 16) all synthesis conditions being identical to those of the IPN synthesis except that no DVB is added. The  $\tan \delta$  peak of the rich PS phase is observed at 128 °C which corresponds to an 15 °C shift compared with the single PS value ( $T_{\alpha} = 113$  °C). The confined PS chains environment inside the PIB network might be responsible for this increase of mechanical relaxation temperature. A similar behavior has been observed for PIB/PMMA IPNs [19].

In order to compare the thermomechanical material properties of the same IPN materials at room temperature, storage modulus  $E'$  and  $\tan \delta$  values at 25 °C are reported in Fig. 13. IPN's storage moduli are weak and increase from 0.65 to 26 MPa when the PS content increases from 0 to 50% by weight. The PS rich phase has little influence on the material rigidity. Accordingly,  $\tan \delta$  is nearly constant and equal to 0.20. Thus these materials show good damping properties and this is in agreement with their flexible macroscopic behavior. In this proportion range (PS content below 50%) IPNs behave like vulcanized rubbers the modulus of which increases with hard

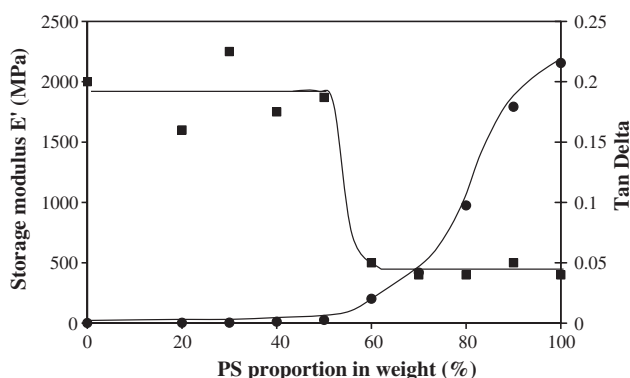


Fig. 13. Storage modulus (●) and  $\tan \delta$  (■) at 25 °C versus PS proportion weight inside PIB/PS IPNs.

filler amount, i.e. PS rich phase domains are dispersed inside a PIB matrix. Poly(styrene-*b*-isobutylene-*b*-styrene) block copolymers which present a micro-phase separation show a similar behavior: the storage modulus increases from 5 to 973 MPa when the PS volume proportion increases from 20 to 55% [2–4]. The TEM analyses of those materials reveal packed cylinders of PS dispersed into hexagonal morphology within a PIB matrix. In the same composition range, the storage moduli of these block copolymers are higher than those of PIB/PS IPN's. Finally, the modulus values measured at 25 °C increase from 200 to 3000 MPa when the PS content increases from 60 to 100%. Simultaneously,  $\tan \delta$  values suddenly decrease until 0.05 that corresponds to the PS single network  $\tan \delta$  value.

Thus, it is possible to improve the PIB network thermo-mechanical properties by combining it with PS inside IPN architecture. First, when the PS weight content is above 50%, IPN storage modulus increases significantly which must be due to PS phase continuity on the whole of the material. However, due to the chosen synthesis pathway, the PIB network is first formed and tends to be continuous in space and for high concentrations of the second polymer, dual phase continuity is likely to occur [6,5]. Thus, the PIB and PS rich phases should be cocontinuous on the whole of the material. Secondly, the PIB damping properties are kept if less than 50% PS weight content is introduced into the IPN. Thus, the PIB network forms the continuous phase on the whole of the material that is always in agreement with the synthesis pathway. On the other hand, the PS rich phase should be dispersed within the PIB matrix. These results are in agreement with the synthesis pathway.

In this study, the PIB network is formed first as shown in the kinetic part study. In this way, when PS is minor component, the PS rich phase should be dispersed within the PIB matrix. On the other hand, when PS is the major compound, 'dual phase continuity' is not an unreasonable hypothesis for the description of these IPNs.

This DMTA analysis enlightens some characteristics of the IPN morphology that have been confirmed by AFM measurements. AFM analyses in tapping mode are performed on two PIB/PS IPN surfaces with different PS weight proportions. The AFM image contrast is given by the stiffness difference between PIB and PS rich phases. Thus the PIB rich phase

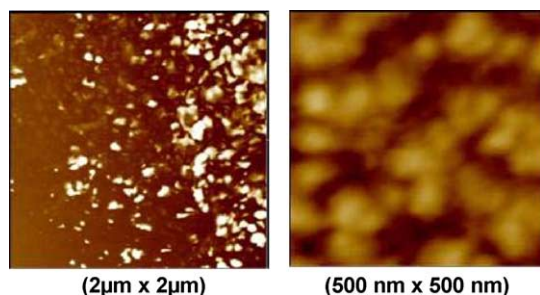


Fig. 14. AFM images of PIB/PS (60:40) IPN-enriched PS phase in white and enriched PIB phase in dark.

appears dark and the PS rich phase appears white on the image. The images of a PIB rich IPN (PIB/PS (60:40) IPN) surface are reported in Fig. 14(a) and (b). The PIB rich phase represents the continuous phase (matrix) in which rich PS nodules are dispersed (clear phase). Whatever the scale of observation, these nodules exhibit various shapes and their size varies from 60 to 100 nm that is in agreement with the phase domain sizes generally reported for IPN materials [43] and with the detection of two mechanical relaxation temperatures by DMTA analysis.

A PS enriched IPN (PIB/PS (20:80) IPN) has been also examined by AFM analysis (Fig. 15(a) and (b)). Although not being the predominant component, the PIB partner still plays the role of the matrix. Indeed, the PIB rich phase (in dark) can be identified as the continuous one over the whole material whatever the observation scale. The PS rich phase appears as dispersed domains with various shapes that seem to result from PS nodules interconnection. Thus this IPN presents also the morphology predicted from DMTA of interconnected PS domains inside a PIB matrix, i.e. a PIB and PS phase cocontinuity. Thus the conclusions which can be drawn from those images are in agreement with the morphology suggested by the thermomechanical properties analysis.

**3.2.2.2. PS cross-linking density effect.** Since two mechanical relaxations corresponding to two phases enriched in one of the two polymers (PIB and PS rich phases respectively) are detected by DMTA, it can be concluded that the IPNs described here show a phase separation. However the phase separation extent might be reduced if the cross-linking density of at least one of both networks is increased [44,45]. For this reason, PS cross-linking density effect on IPN thermomechanical

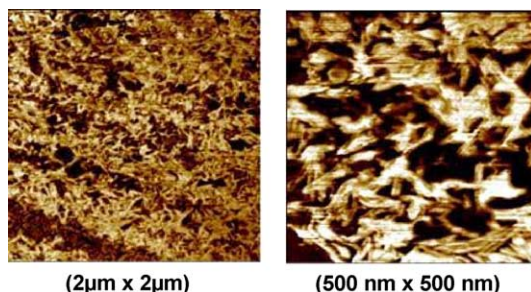


Fig. 15. AFM images of PIB/PS (20:80) IPN-enriched PS phase in white and enriched PIB phase in dark.

properties has been studied on IPNs with various PIB/PS weight proportions. Except for the DVB amount that controls the cross-linking density of the PS network, the other network synthesis conditions are kept identical.

In a first step, PIB/PS (70:30) IPNs in which PIB is the main component have been synthesized with different DVB weight proportions with respect to styrene (from 0 to 30%) and further characterized by DMTA. The storage moduli and PIB  $\tan \delta$  peak of this series of IPNs are only slightly affected by the PS cross-linking density compared with the storage modulus measured previously (11% DVB by weight with respect to styrene). The PS cross-linking density increase mainly acts on the PS rich phase. Although the PS mechanical relaxation is undetectable for this weight proportion it might indirectly be reflected on the behavior of the PIB rich phase. Thus PS is present in the PIB rich phase but does not form a continuous phase over the whole material considering the low modulus values measured at temperatures higher than that of PIB mechanical relaxation. Those observations are in agreement with the macroscopic response of the IPNs which behave as reinforced rubbers.

In a second step, the thermomechanical properties of PIB/PS (30:70) IPNs in which PS is the main component and the DVB amount varies from 0 to 30% by weight with respect to styrene are shown in Fig. 16. The two mechanical relaxations are always present whatever the PS cross-linking density used. Thus the increase in cross-linker proportion does not allow suppression of phase separation but affects the PIB/PS (30:70) IPN thermomechanical properties. The intermediate plateau position and the storage modulus values after PS mechanical relaxation temperature increase with the cross-linker density. For example the storage modulus plateau value of the IPN containing 30% DVB is 35 times higher than that of the semi-IPN (without DVB, i.e. with no cross-links at all) at 25 °C. Thus the increase of PS cross-linking density indeed affects both the PS rich phase and the whole material properties.

The PS cross-linking density has also an important influence on  $\tan \delta$  curves. The  $\tan \delta$  peak height at  $-30$  °C corresponding to PIB mechanical relaxation decreases when the DVB amount increases from 0 to 20% but the shoulder at  $-50$  °C is hardly affected. The PIB cooperative backbone *gauche-trans* skeletal movements are more hindered by the PS cross-linking density increase than the PIB local rotational chain movements. The same behavior has been observed when the PS weight proportion increases (DVB keeping constant) for PIB/PS IPNs mainly composed of PIB. Simultaneously, the PS rich phase mechanical relaxation peak becomes broader, its height decreases and it is shifted towards higher temperatures. This shift is characteristic of a phase with enhanced cross-linking density.

The PS network cross-linking density increase makes rigid both the PS rich phase and the whole material because IPN modulus values before the PS mechanical relaxation also increase. This result is in agreement with a PS rich phase cocontinuous on the whole material.

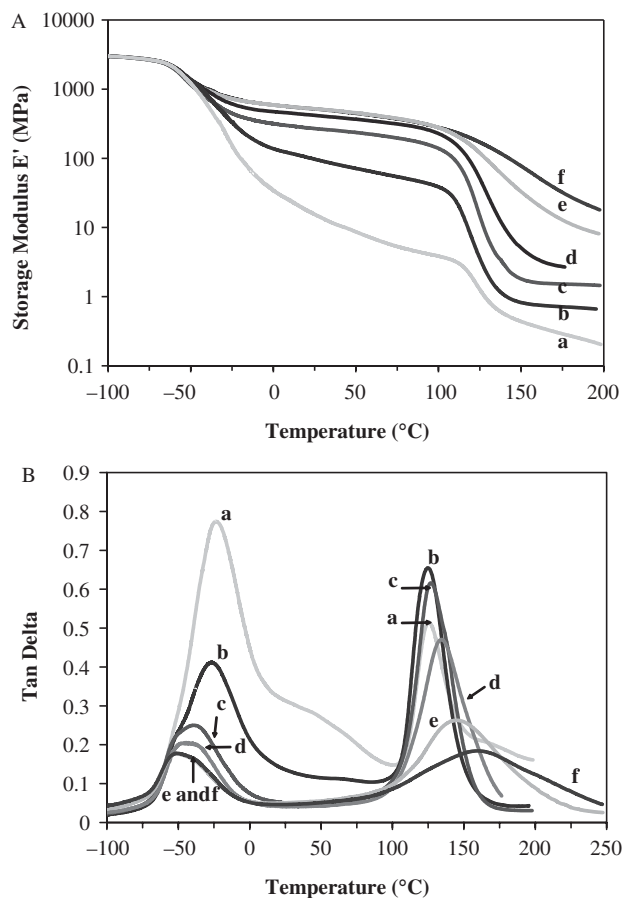


Fig. 16. (A) Storage modulus and (B)  $\tan \delta$  versus temperature for PIB/PS (30:70) IPN synthesized with different DVB content (% w/w styrene): 0% (a), 1% (b), 5% (c), 11% (d), 20% (e) 30% (f).

In conclusion, due to the morphology change, the material rigidity and damping properties depend on the IPN composition. However, a higher rigidity (higher storage modulus) is associated with lower damping properties (lower  $\tan \delta$  values). Thus, the PS weight content has to be chosen according to the properties one would like to obtain.

### 3.2.3. Tensile properties

Fig. 17 displays representative stress–strain curves for the IPNs with different PS weight proportions. No elongation at break has been obtained under these conditions (low force tract apparatus 18N and short maximum distance between clamps stop the run). Nevertheless the results show that the properties of PIB/PS IPNs range from an elastomer (the strain at break is over 100%) when PIB is the major component, to that of a ductile thermoset when PIB is the minor component. The tensile properties of the IPNs clearly depend on the IPN architecture. The stress and the strain at break are equal to 8 MPa and 10% respectively for PIB/PS (40:60) IPN. The poly(styrene-*b*-isobutylene-*b*-styrene) block copolymer containing 41% volume PS shows a stress and a strain at break of 15 and 372%, respectively [2]. These results are however difficult to compare because the measurements have not been

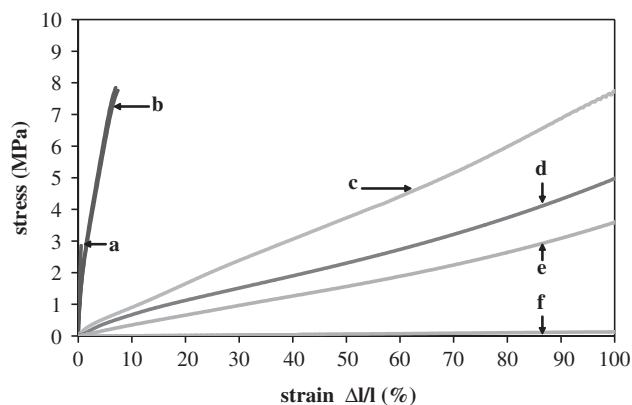


Fig. 17. Strain–stress curves of 30:70 (a), 40:60 (b), 50:50 (c), 60:40 (d), 70:30 (e) PIB/PS IPNs and (f) PIB single network. Deformation rate: 1 mm/min.  $T=35^{\circ}\text{C}$ .

carried out in the same experimental conditions (strain rate, temperature,...).

The Young moduli  $E$  values estimated from the slope at the origin of the previous curves increase with the PS content in the materials. Indeed, the Young modulus is about 2, 16 and 630 MPa for (70/30) PIB/PS IPN, (50:50) PIB/PS IPN and (30:70) PIB/PS IPN, respectively. The Young's modulus measured on PS–PIB–PS block copolymers increases from 1 to 60 MPa when the PS volume content increases from 22 to 45% [2]. Thus Young's moduli of IPNs are higher than those of copolymers. This difference should be due to the particular and previously explained PS distribution inside the IPN architecture according to its weight proportion.

### 3.3. IPN ageing

The IPN architecture should lead to a protection of each individual network from the physical and/or chemical attacks. The single PIB and PS networks and the PIB/PS IPNs are exposed to UV in order to promote their ageing. The material absorbance is measured at 350 nm every 24 h in order to estimate the ageing behavior. The ratio of the absorbance variation ( $A_t - A_0$ ) and the initial absorbance ( $A_0$ ) versus time curves are shown in Fig. 18.

The single PS network is much more sensitive to UV irradiation than the single PIB one or PIB/PS IPNs. Indeed, the PS single network absorbance is multiplied by 9 after 120 h and the material turns yellow contrary to single PIB network and IPNs whose absorbance hardly doubled. Aromatic compounds are well known to lead to yellowish material following UV irradiation. The difference of absorbance variations between the single networks and IPNs is not due to a dilution effect as IPN absorbance variations are lower than those of the single networks. The PS phase inside the IPN architecture is thus protected from irradiation.

In conclusion, the weak UV ageing of IPN and semi-IPN must be pointed out. The PS phase introduced in these materials degrades much less and seems to be protected inside the IPN architecture. This phenomenon has been confirmed by the DMTA analysis carried out on IPNs and semi-IPNs before

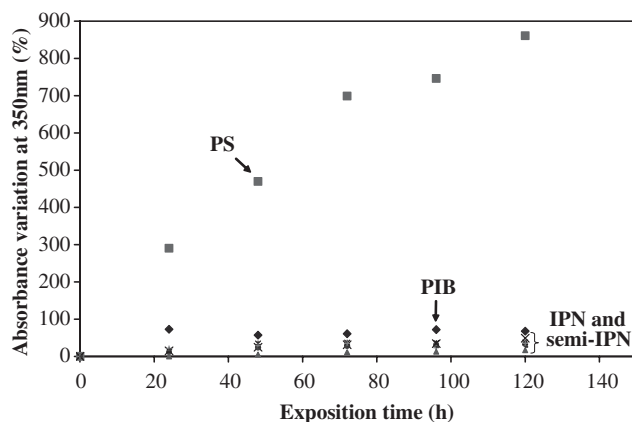


Fig. 18. Single PIB and PS networks and IPN absorbance variation measured at 350 nm versus time under UV exposure.

and after UV exposure. Their thermomechanical properties are unchanged after 140 h. Whereas, PS single network undergoes a post-cross-linking process ( $\alpha$  relaxation shifted to higher temperature) and PIB single network undergoes chain scission (increased  $\tan \delta$  values on the rubbery plateau).

#### 4. Conclusion

The synthetic pathways leading to polyisobutene and polystyrene based IPNs have been studied. The synthesis involves an in situ process in which all components are first mixed together without solvent. The synthesis conditions have been determined in order to obtain the higher interpenetration degree of the partner networks. The network formations inside the IPN architecture have been investigated by near FTIR spectroscopy. Thus, the change of nature and amount of the PS network initiator in the initial mixture makes it possible to accelerate or slow down the PS network formation compared to the PIB network one which is unchanged. Thus 0.5% BPO by weight with respect to styrene is used when PIB network is first formed and a transparent material is obtained. In order to synthesize networks quasi-simultaneously, 5% BPO are introduced in the medium; the obtained IPN is translucent. Finally, 5% DCPD leads to the PS network formation before PIB one; in this last case, the PIB network is opaque and its formation has not been completed, the PS network formation hindering the PIB network one.

In order to examine the network interpenetration, mechanical properties of the resulting materials have been studied by DMTA. All IPNs show two distinct mechanical relaxations at about  $-30$  and  $+100$  °C corresponding to PIB rich phase and PS rich one respectively. These studies have shown that the interpenetration degree between two networks in an interpenetrating polymer network structure could be improved changing the network formation order. It was shown that the best interpenetrating degree in these IPNs was achieved when PIB network is first synthesized. A PIB network swollen by styrene is obtained as an intermediate state and the PS network is subsequently synthesized inside this PIB network.

The morphologies and the thermomechanical properties of PIB/PS IPNs were studied for different weight proportions and cross-linking densities of the PS network. DMTA measurements and AFM microscopy have shown that the material morphology mainly depends on the weight proportion of each component. When the PIB network is the main component, it forms the matrix in which are dispersed PS rich domains. The resulting material has reinforced elastomeric properties. PIB and PS phase cocontinuity is observed when the IPN is mainly composed of PS. The material is, in this case, rigid. In all cases, the mechanical properties and the UV ageing resistance of the IPNs are tremendously improved by the introduction of a PS network in the IPN architecture, which was indeed the aim of this work.

#### Acknowledgements

The authors thank BASF for financial support, and particularly Dr H.-P. Rath who very actively supported this research and also provided the  $\alpha,\omega$ -dihydroxy polyisobutene samples. They also thank Dr R. Blackborow for many stimulating discussions and Drs F. Vidal and B. Amana from university of Cergy-Pontoise for assistance in carrying out the DMTA analysis and AFM measurements, respectively.

#### References

- [1] Othmer K. Encyclopedia of chemical technology. New York: Wiley; 1998.
- [2] Storey RF, Chisholm BJ, Masse MA. *Polymer* 1996;37(14):2925–38.
- [3] Storey RF, Baugh DW. *Polymer* 2001;42(6):2321–30.
- [4] Storey RF, Baugh DW. *Polymer* 2000;41(9):3205–11.
- [5] Sperling LH, Mishra V. IPNs around the world: science and engineering. New York: Wiley; 1997 p. 1–25.
- [6] Sperling LH. In: Sperling LH, Klemmner D, Utracki LA, editors. Interpenetrating polymer networks. Advances in chemistry series, vol. 239. Washington, DC: American Chemical Society; 1994. p. 3–38.
- [7] Sherman MA, Kennedy JP, Ely DL, Smith D. *J Biomater Sci Polym* 1999; 10(3):259–69.
- [8] Sherman MA, Kennedy JP. *J Polym Sci, Part A* 1998;36:1901–10.
- [9] Sherman MA, Kennedy JP. *J Polym Sci, Part A* 1998;36:1891–9.
- [10] Ivan B, Almdal K, Mortensen K, Johannsen I, Kops J. *Macromolecules* 2001;34(6):1579–85.
- [11] Erdodi G, Ivan B. *Chem Mater* 2004;16(6):959–62.
- [12] Janecska A, Ivan B. *Polym Mater Sci Eng* 1998;79:477–8.
- [13] Fu FS, Mark JE. *J Appl Polym Sci* 1989;37(9):2757–66.
- [14] Widmaier JM, Drillières S. *J Appl Polym Sci* 1996;63(7):951–8.
- [15] Zhou P, Frisch HL. *Macromolecules* 1994;27(7):1788–94.
- [16] Suthar B, Xiao HX, Klemmner D, Frisch KC. IPNs around the world: science and engineering. New York: Wiley; 1997 p. 49–73.
- [17] Lipatov YS, Alekseeva T. IPNs around the world: science and engineering. New York: Wiley; 1997 p. 75–93.
- [18] Ni H, Aaserud DJ, Simonsick Jr WJ, Soucek MD. *Polymer* 2000;41(1): 57–71.
- [19] Vancaeyzeele C, Fichet O, Boileau S, Teyssié D. *Polymer* 2005;46(18): 6888–96.
- [20] Vancaeyzeele C. PhD Thesis. Cergy-Pontoise University; 2004.
- [21] Fichet O, Vidal F, Laskar J, Teyssié D. *Polymer* 2005;46(1):37–47.
- [22] Teyssié D, Vancaeyzeele C, Laskar J, Fichet O, Boileau S, Blackborow R, Rath HP, Lange A, Lang G, Mach H, Hiller M. Molding compound. Patent number WO2005019285; 2005.
- [23] Zetterlund PB, Yamazoe H, Yamada B. *Polymer* 2002;43(25):7027–35.

- [24] Schapman F, Couvercelle JP, Bunel C. *Polymer* 1998;39(4):965–71.
- [25] Laskar J, Vidal F, Fichet O, Gauthier C, Teyssié D. *Polymer* 2004;45(15):5047–55.
- [26] Odian G. *Principle of polymerization*. 3rd ed. New York: Wiley; 1991.
- [27] Fontanille M, Gnanou Y. *Chimie et physico-chimie des polymères*. Paris: Dunod; 2002 p. 244.
- [28] Schapman F, Couvercelle JP, Bunel C. *Eur Polym J* 2002;38(10):1979–86.
- [29] Deschères I, Pham QT. *Makromol Chem* 1987;188(10):1909–22.
- [30] Grigor'eva VA, Baturin SM, Entelis SG. *Vysokomol Soedin A* 1972;14(6):1345–9.
- [31] Zabrodin VB, Nesterov OV, Entelis SG. *Kinet Katal* 1970;11(4):1060–2.
- [32] Hua FJ, Hu CP. *Eur Polym J* 1999;35(1):103–12.
- [33] Ruzette AVG, Mayes AM. *Macromolecules* 2001;34(6):1894–907.
- [34] Zhou P, Xu Q, Frisch HL. *Macromolecules* 1994;27(4):938–46.
- [35] Brandrup J, Immergut EH, Grulke EA. *Polymer handbook*. 4th ed. New York: Wiley; 1999.
- [36] Puskas JE, Antony P, El Fray M, Altstädt V. *Eur Polym J* 2003;39(10):2041–9.
- [37] Plazek DJ, Chay IC, Ngai KL, Roland CM. *Macromolecules* 1995;28(19):6432–6.
- [38] Ngai KL, Plazek DJ. *Macromolecules* 2002;35(24):9136–41.
- [39] Frick B, Richter D. *Phys Rev B* 1993;47(22):14795–804.
- [40] Noshay A, McGrath JE. *Block copolymer: overview and critical survey*. New York: Academic Press; 1977 [chapter 4].
- [41] He XW, Widmaier JM, Herz JE, Meyer JC. *Polymer* 1992;33(4):866–71.
- [42] Tabka MJ, Widmaier JM, Meyer JC. *Sound and vibration damping with polymers*. Washington, DC: ACS; 1990.
- [43] Qin CL, Cai WM, Cai J, Tang DY, Zhang JS, Qin M. *Mater Chem Phys* 2004;85(2/3):402–9.
- [44] Zhou P, Frisch HL, Rogovina L, Makarova L, Zhdanov A, Sergeienko N. *J Polym Sci, Part A* 1993;31(10):2481–91.
- [45] Wang SH, Zawadzki S, Akcelrud L. *J Polym Sci, Part B* 2000;38(22):2861–72.